ACI MATERIALS JOURNAL TECHNICAL PAPER

Title No. 116-M05

Artificial Intelligence to Investigate Modulus of Elasticity of Recycled Aggregate Concrete

by Seyedhamed Sadati, Leonardo Enzo Brito da Silva, Donald C. Wunsch II, and Kamal H. Khayat

*Modulus of elasticity (MOE) is one of the main factors that affect the deformation characteristics and serviceability of concrete in the hardened state. The use of recycled concrete aggregate (RCA) in concrete production can lead to a significant reduction in the MOE. An artificial neural network (ANN) was employed to quantify the effect of coarse RCA on the concrete's MOE. A database summarizing over 480 data series obtained from 52 technical publications was developed and analyzed using ANN. Concrete mixture proportions and aggregate properties were considered input parameters. The rate of reduction in 28-day MOE was considered the output parameter. An additional data set of 43 concrete mixtures obtained from laboratory investigation of concrete with well-known properties was used to validate the established model. Several combinations of input parameters and ANN architectures were considered in the analysis. Results indicated that the performance of the system was acceptable, with a coefficient of correlation ranging from 0.71 to 0.95 for the training, validation, and testing of the model with a mean square error limited to 0.008. The developed model was incorporated for a case study on a typical concrete used for rigid pavement construction. Contour graphs were developed to showcase the effect of up to 100% coarse RCA replacement on the variations in the MOE of concrete made with 0.40 water-cementitious materials ratio (*w/cm*) and 323 kg/m³ (545 lb/yd³) of a binary cement, designated for rigid pavement construction. The results indicated that depending on the RCA quality, a reduction of 10 to 30% in the MOE of pavement concrete made with 50% RCA can be expected. However, the reduction in the MOE will be limited to 10% when RCA with water absorption limited to 2.5% and an oven-dry specific gravity of over 2500 kg/m³ (156 lb/ft³) is used.*

Keywords: artificial intelligence; machine learning; modulus of elasticity; neural networks; recycled concrete aggregate; sustainable infrastructure.

INTRODUCTION

Construction and demolition (C&D) waste accounts for a considerable portion of solid wastes with an increasing rate of generation in the United States. The total amount of C&D waste was estimated to be over 325 million tons in the United States in 2003.[1] More recent estimates by the Environmental Protection Agency (EPA) indicate that over 530 and 535 million tons of C&D waste was generated in the United States in 2013 and 2014, respectively, with concrete constituting about 70% of the C&D waste.[2,3] Historically, concrete from C&D waste has mostly been dealt with through disposal in landfills. The environmental impacts, raising issues with the depletion of virgin aggregate, more restrictive landfill policies, and the potential savings in construction costs associated mainly with reduced hauling distances, support the idea of seeking alternative applications for C&D waste. One of the main ideas is to turn the waste concrete into an added value material—recycled concrete aggregate (RCA)—for use as a replacement of the virgin aggregate in concrete construction.[4,5]

The performance of concrete made with RCA can be impacted when using RCA materials of inferior quality compared to that of virgin aggregate. The MOE is one of the characteristics of concrete that can be highly sensitive to the incorporation and quality of RCA. The availability of residual mortar in RCA particles can reduce the overall stiffness and restraining capacity of the coarse-aggregate skeleton and increase the absolute volume of mortar in the hardened state. This reduces the rigidity of the concrete, resulting in a lower MOE compared to the corresponding mixtures prepared without any RCA. Moreover, the presence of microcracks in the residual mortar, old virgin aggregate, and the old interfacial transition zone (ITZ) between these two phases (anticipated due to the crushing procedure) can affect the MOE significantly.[6] Several sources in the technical literature indicate a significant reduction in MOE due to the RCA incorporation.[5,7-9]

Traditionally, the MOE of concrete is considered to depend on the compressive strength, unit weight, and type of aggregate in use. For example, the European standard[10] considers the MOE as a function of compressive strength, with estimated values for each strength category presented in tabular format. The Japanese standard[11] uses a tabular format to estimate the MOE for two main concrete categories: 1) normal-aggregate concrete; and 2) lightweight-aggregate concrete. The American Concrete Institute (ACI)[12] considers two equations for estimating the MOE as a function of compressive strength: 1) Eq. (1) for lightweight concrete with a unit weight of 1440 to 2560 kg/m³ (90 to 160 lb/ft³); and 2) Eq. (2) for normalweight concrete. The equations are as follows

$$E_c = (0.043\sqrt{f_c'})(W_c)^{1.5} \quad (1)$$

$$E_c = 4700\sqrt{f_c'} \quad (2)$$

where W_c is the unit weight of the concrete, kg/m³; and f_c' is the compressive strength, MPa.

ACI Materials Journal, V. 116, No. 1, January 2019.

MS No. M-2018-029.R1, doi: 10.14359/51706948, was received February 18, 2018, and reviewed under Institute publication policies.

Behnood et al.[13] indicated that the abovementioned models cannot accurately predict the MOE of concrete made with RCA. Given the importance of the issue, considerable efforts have been devoted to quantifying the effect of RCA on MOE. Examples of such models are provided in Eq. (3) to (10), developed by Ravindrarajah and Tam,[14] Dhir et al.,[15] Dillmann,[16] Mellmann,[17] Kakizaki et al.,[18] Zilch and Roos,[19] Corinaldesi,[20] and Xiao et al.,[21] respectively

$$E_c = 4.63 f_{cy}^{0.50} \quad (3)$$

$$E_c = 0.37 f_c + 13.1 \quad (4)$$

$$E_c = 0.63443 f_{cu} + 3.0576 \quad (5)$$

$$E_c = 0.378 f_c + 8.242 \quad (6)$$

$$E_c = 190(\rho/2300)^{1.5}\sqrt{(f_{cu}/2000)} \quad (7)$$

$$E_c = 9.1(f_{cu} + 8)^{1/3} \times (\rho/2400)^2 \quad (8)$$

$$E_c = 18.8(0.83 f_{cu}/10)^{1/3} \quad (9)$$

$$E_c = 100/(2.8 + 40.1/f_{cu}) \quad (10)$$

where E_c is the MOE of concrete, GPa; f_c is the compressive strength, MPa; and ρ is the unit weight of concrete, kg/m^3.

However, considering the limitations associated with the experimental domain investigated in each case, and due to the variable nature of RCA materials, the available analytical models still need to be expanded. Examples of such models can be found in the literature where mechanical properties of concrete made with RCA were investigated using deep learning and soft computing.[13,22,23] The research presented in this paper establishes a model to estimate the MOE of concrete made with coarse RCA that is based on the artificial neural network (ANN) method. A wide range of mixture design parameters, including the binder type and content, water content, virgin aggregate properties and content, and RCA characteristics and content are considered as input parameters. The extent of the variation in MOE due to RCA use was the output. A database was developed and analyzed to establish a prediction model. Given the wide range of investigated parameters, the model is intended to estimate the effect of RCA on the MOE of concrete designated for a variety of applications, including infrastructure construction.

RESEARCH SIGNIFICANCE

Given the variable nature of RCA materials, there exists the need to have predictive tools that enable reliable estimations for properties of concrete made with RCA, including the MOE. Developing the model to estimate variations in the MOE of concrete involved three main phases. The first phase included the development and screening of a database of published literature on the MOE of concrete made with coarse RCA. The second phase was to generate laboratory data to validate the model. The third phase involved testing the model based on ANN.

EXPERIMENTAL PROGRAM

Development and analysis of database

The database that was established to correlate the MOE of concrete with the key parameters affecting it consisted of 484 data series obtained from 52 published articles.[4,7-9,20,24-70] The 28-day compressive strength of the investigated concrete mixtures ranged from a minimum of 15 MPa to approximately 110 MPa (2175 to 15,950 psi). The minimum and the maximum MOE values were 11 and 55 GPa (1595 and 8000 ksi), respectively. Each dataset included a summary of the concrete mixture design, virgin aggregate content and properties, and coarse RCA content and characteristics. The investigated input factors are elaborated as follows.

Binder: Binder content (kg/m^3) and binder type, which was considered as a categorical factor of 1 or 2. An input value of 1 was attributed to the concrete with plain portland cement (OPC), while binder type 2 was used for concrete mixtures with supplementary cementitious materials (SCMs).

Water: water-binder ratio (w/b), water-cement ratio (w/c), and water content (kg/m^3).

Fine aggregate: Fine aggregate content (kg/m^3).

Virgin coarse aggregate: Virgin coarse aggregate content (kg/m^3), virgin coarse aggregate water absorption (%), virgin coarse aggregate oven-dry specific gravity, and virgin coarse aggregate Los Angeles (LA) abrasion value (%).

Coarse RCA: Coarse RCA (C-RCA) content (kg/m^3), coarse RCA water absorption (%), coarse RCA oven-dry specific gravity, coarse RCA LA abrasion value (%), and coarse RCA replacement ratio (% mass).

Total coarse aggregate: Total coarse aggregate content (kg/m^3), combined coarse aggregate water absorption (%), combined coarse aggregate oven-dry specific gravity, and combined coarse aggregate LA abrasion value (%). The combined coarse aggregate properties were calculated as a linear combination of the properties and relative mass of the blend constituents, as proposed by Omary et al.[71] Equations (11), (12), and (13) were used to determine the oven-dry specific gravity, water absorption, and mass loss due to LA abrasion, respectively, of a given combination of coarse aggregate, respectively, as suggested by Omary et al.[71]

$$Coarse_{SG} = [(Mass_{RCA} \times RCA_{SG}) + (Mass_{NC} \times NC_{SG})]/(Mass_{RCA} + Mass_{NC}) \quad (11)$$

$$Coarse_{Abs} = [(Mass_{RCA} \times RCA_{Abs}) + (Mass_{NC} \times NC_{Abs})]/(Mass_{RCA} + Mass_{NC}) \quad (12)$$

$$Coarse_{LA} = [(Mass_{RCA} \times RCA_{LA}) + (Mass_{NC} \times NC_{LA})]/(Mass_{RCA} + Mass_{NC}) \quad (13)$$

where $Mass_{RCA}$ is the RCA content (kg/m^3); $Mass_{NC}$ is the virgin coarse aggregate content (kg/m^3); RCA_{SG} is the oven-dry specific gravity of RCA; NC_{SG} is the oven-dry specific gravity of the virgin coarse aggregate; RCA_{Abs} is the water absorption of the RCA (%); NC_{Abs} is the virgin coarse aggregate absorption rate (%); RCA_{LA} is the mass loss due to LA abrasion of RCA (%); NC_{LA} is the mass loss due to LA abrasion of the virgin coarse aggregate (%); and $Coarse_{SG}$, $Coarse_{Abs}$, and $Coarse_{LA}$ are the oven-dry specific gravity,

Table 1—ANN model input and output parameters for database and laboratory mixtures

		Parameter	Database				Laboratory				Scenario			
			Min.	Max.	Avg.	Std. dev.*	Min.	Max.	Avg.	Std. dev.*	I	II	III	IV
Input parameters	1	Binder content, kg/m^3	210	609	375.2	65.5	317	323	322	2	●	●	●	●
	2	Binder type	1: OPC	2: SCM	—	—	2	2	—	—	●	●	●	●
	3	Virgin coarse content, kg/m^3	0	1950	558.0	444.0	0	1136	632	310	●	●	●	●
	4	Coarse RCA content, kg/m^3	0	1800	501.9	435.0	0	964	410	260	●	●	●	●
	5	Water-binder ratio (w/b)	0.25	0.87	0.48	0.11	0.37	0.45	0.40	0.02	●	●	●	●
	6	Water-cement ratio (w/c)	0.29	1.22	0.52	0.14	0.53	0.80	0.63	0.11	●	●	●	●
	7	Fine aggregate content, kg/m^3	465	1301	726	126	772	795	785	7	●	●	●	●
	8	Coarse aggregate absorption, %	0.20	6.10	1.26	0.80	0.50	0.98	0.80	0.10	●	●	●	●
	9	C-RCA absorption, %	1.93	18.91	5.39	2.41	4.20	7.58	5.40	1.17	●	●	●	●
	10	Coarse specific gravity, OD, kg/m^3	2483	2880	2607	82	2640	2730	2719	23	●	●	●	●
	11	C-RCA specific gravity, OD, kg/m^3	1800	2602	2313	125	2170	2380	2297	73	●	●	●	●
	12	Coarse aggregate NMAS, mm	8	32	20.1	4.0	19	19	19	0	●	●	●	●
	13	Coarse RCA NMAS, mm	8	32	19.0	4.9	13	19	18	2	●	●	●	●
	14	Coarse aggregate LA abrasion, %	14	43	20.8	6.0	24	43	29.3	5.1			●	●
	15	C-RCA LA abrasion, %	13.7	81.7	33.8	8.8	33	53	39.3	6.2			●	●
	16	Water content, kg/m^3	108	234	175	30	120	143	128	7		●		●
	17	Total coarse aggregate content, kg/m^3	640	1950	1060	143	907	1136	1042	53		●		●
	18	Coarse combination absorption, %	0	16	3.2	2.0	0.50	7.13	2.70	1.40		●		●
	19	Coarse combination specific gravity, OD	1800	2880	2467	144	2210	2730	2543	123		●		●
	20	Coarse combination LA abrasion, %	13.7	51.5	27	8	24	53	33.5	5.5				●
	21	Coarse RCA replacement ratio	0	1	0.5	0.4	0	1	0.4	0.3		●		●
Output		Relative MOE (R_{MOE})	0.44	1.37	0.89	0.12	0.67	1.05	0.89	0.09				

*Standard deviation.

Note: 1 kg/m^3 = 1.686 lb/yd^3.

water absorption rate (%), and LA abrasion (%) of the coarse aggregate combination, respectively.

Table 1 offers a summary of the input features along with the corresponding minimum and maximum values. Four different scenarios of input factors were explored to ensure the most generalized and robust predictions with the lowest chance of overfitting the data. Development of a comprehensive model requires employment of user-friendly, yet representative, indexes to depict the RCA quality. One should note that the heterogeneous nature of RCA makes it impossible to define representative indexes at the microlevel. Therefore, the considered RCA properties included water absorption, specific gravity, and mass loss due to LA abrasion, which are also employed by the standards, recommendations, and guidelines to define RCA quality.[72] The investigated input scenarios are elaborated in the following and summarized in Table 1.

Scenario I—The input factors included 13 independent properties summarizing the key mixture design details, virgin aggregate properties, and RCA characteristics. The aggregate-related properties included the aggregate content (kg/m^3), oven-dry specific gravity, and water absorption (%) for both the virgin and RCA materials. The LA abrasion value was not included in the first scenario because not all the investigated sources from the literature reported these values for RCA.

Scenario II—A total number of 18 input factors were investigated for the second scenario. The input parameters included the 13 independent properties (elaborated on in Scenario I) and an additional set of five dependent parameters. The aggregate-related properties considered in the second scenario included the aggregate content (kg/m^3), oven-dry specific gravity, and water absorption (%) for both the virgin and RCA materials. Again, the LA abrasion of the coarse virgin aggregate and RCA were not included in the analysis. The additional dependent variables were the total water content in the mixture, total coarse-aggregate content (kg/m^3), RCA replacement ratio (% mass) of coarse aggregate, combined coarse aggregate oven-dry specific gravity, and combined coarse aggregate water absorption (%); the last two values were calculated using Eq. (11) and (12), respectively.

Scenario III—A total number of 15 independent input parameters were considered for the third scenario. The 13

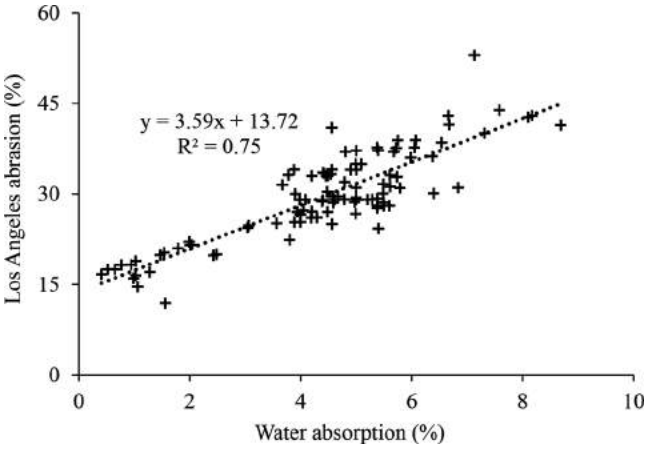

Fig. 1—Correlation between LA abrasion and water absorption.

factors elaborated on Scenario I were incorporated along with the LA abrasion values of the virgin coarse aggregate and the RCA materials. As stated earlier, not all the investigated references reported the LA values of the aggregate. Therefore, based on the data reported in the literature, in addition to a laboratory investigation that was undertaken herein, correlations were established between the LA abrasion and the water absorption and specific gravity of the RCA as suggested by González-Taboada et al.[73] Figure 1 presents the correlations between the LA abrasion and the water absorption developed by González-Taboada et al.[73] and further updated by the authors obtained from over 100 different RCA types. A strong linear correlation was observed, with a R^2 value of 0.75 for the relationship between the LA abrasion and the water absorption. The correlation established in Fig. 1 was employed to estimate the LA abrasion for concrete mixtures where actual values were missing data points of the database.

Scenario IV—A total number of 21 input parameters were included in this scenario. The aggregate-related properties considered in this scenario included the aggregate content (kg/m^3), oven-dry specific gravity, water absorption (%), and LA abrasion (%) for both the virgin and RCA materials. The additional dependent variables were the water content in the mixture, total coarse aggregate content (kg/m^3), RCA replacement ratio (% mass), combined coarse aggregate water absorption (%), combined coarse aggregate oven-dry specific gravity, and combined coarse aggregate LA abrasion (%) calculated using Eq. (11), (12), and (13), respectively.

Output—The output of the study was the relative variation in MOE, defined in Eq. (14)

$$R_{MOE} = \frac{\text{MOE of concrete made with RCA}}{\text{MOE of corresponding reference concrete made without RCA}} \quad (14)$$

A relative performance value of 1.0 was considered for the control mixture (proportioned without any RCA) of each study reported in the database. Considering the relative MOE (R_{MOE}) as the means of comparison reduces the uncertainties related to non-uniform experimental conditions—for example, air content in the hardened state, specimen size, test device, loading rate, and test protocol—typical of database analysis. This way, one can assume that there are no significant correlations between the aforementioned factors and the relative performance of the mixtures.

Laboratory investigation

Material properties—In total, 43 different concrete mixtures were produced in the laboratory. Type I/II portland cement, Class C fly ash (FA-C), and ground-granulated blast furnace slag (GGBS) were used as binder materials. The mixtures were proportioned with either binary or ternary cement. The binary cement was composed of 75% (by mass) OPC and 25% FA-C. The ternary system incorporated 35% FA-C and 15% GGBS. The binary cement was adopted from the concrete mixture design employed by the Missouri Department of Transportation (MoDOT) for rigid pavement construction.[72] The ternary system was optimized based on the mechanical properties and shrinkage of concrete equivalent mortar prepared with a water-cementitious materials ratio (*w*/*cm*) of 0.40, developed by Khayat and Sadati.[72] Three different *w*/*cm* of 0.37, 0.40, and 0.45 were considered during the design of the concrete mixtures. Coarse RCA procured from six different sources, including five recycling centers and one laboratory produced RCA, were considered. A siliceous river sand was incorporated as fine aggregate. Table 2 summarizes the aggregate properties. An air-entraining agent was used to secure 6% ± 1% air in fresh concrete. A water-reducing admixture was incorporated to adjust the initial slump values. Table 1 details the properties of the mixture investigated in laboratory.

Concrete preparation and testing—A drum mixer with 110 L capacity was used for concrete mixing. Slump and air content in the fresh state were determined according to ASTM C143[74] and ASTM C231,[75] respectively. Cylindrical specimens measuring 100 x 200 mm (4 x 8 in.) were employed to determine the compressive strength[76] and MOE.[77] A vibrating table was employed to secure proper consolidation of the concrete. Extracted samples were then covered with wet burlap and plastic sheets up to 24 hours after casting. The specimens were cured in lime-saturated water at 21 ± 2°C (70 ± 3.6°F) up to the testing time at 28 days. Table 1 summarizes the properties of the investigated mixtures.

Model development

Being inspired by biological nervous system, the ANNs are information analysis paradigms that are widely used as computational tools. Concretely, an ANN is a universal function approximator that builds the mapping between an input and an output space. Modeling using ANN involves five main steps: 1) representing the problem and acquiring the data; 2) defining the architecture; 3) determining the learning process; 4) training the network; and 5) testing the developed network to ensure robustness and generalization.[78] Neural networks are composed of a large number of interconnected artificial processing units, known as neurons. Usually, these neurons are arranged in layers (input, hidden, and output), which in turn are fully connected; the number of

Table 2—Properties of aggregate used in laboratory investigation

Aggregate	Source	Specific gravity, kg/m^3	Absorption, %	Los Angeles abrasion loss, %	NMAS, mm
Virgin coarse 1	Crushed dolomite	2730	0.80	28	19
Virgin coarse 2	Crushed dolomite	2720	0.98	43	19
Virgin coarse 2	Crushed limestone	2640	0.50	24	19
Virgin fine	Riverbed sand	2630	0.40	—	4
RCA 1	Laboratory-produced RCA	2350	4.56	41	19
RCA 2	Waste airfield concrete, Missouri	2350	4.46	33	19
RCA 3	Waste airfield concrete, Missouri	2380	4.20	33	19
RCA 4	Unknown concrete waste, Missouri	2250	5.75	39	19
RCA 5	Unknown concrete waste, Kansas	2240	6.05	38	19
RCA 6	Unknown concrete waste, Missouri	2170	7.58	44	19
RCA 7	Unknown concrete waste, Missouri	2210	7.13	53	12.5

Notes: 1 mm = 0.0394 in.; 1 kg/m^3 = 1.686 lb/yd^3.

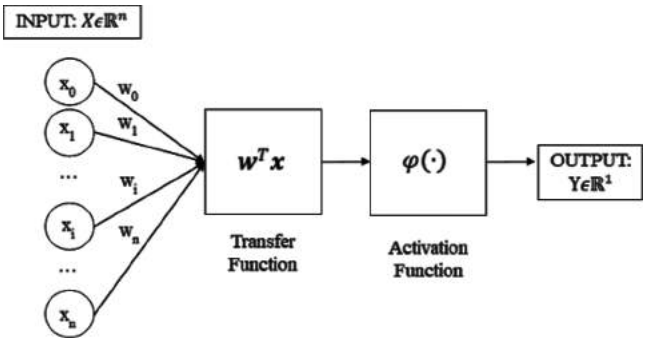

Fig. 2—Schematic structure of simple neuron model.

neurons per layer defines the ANN architecture. Each neuron typically consists of five different parts: inputs, weights, transfer function, activation function, and output, as illustrated in Fig. 2. The transfer function used in this study is the weighted sum presented in Eq. (15)

$$net_j = \boldsymbol{w}^T \boldsymbol{x} = \sum_{i=0}^{n} w_{ij} x_i \tag{15}$$

where $\boldsymbol{x}$ represents the input vector applied to a given neuron associated with weight vector $\boldsymbol{w}$; thus, net_j is the weighted sum of the j-th neuron based on its weights and input values from n neurons of the preceding layer; w_{ij} is the weight factor between the j-th neuron and the i-th neuron of the preceding layer, whose output is x_i, and $b = w_{0j}x_0$ is the bias ($x_0 = 1$).

The activation function $\varphi(\cdot)$ translates the *net* value to the neuron output. A variety of activation functions were presented in the literature, such as linear, sigmoid, and hyperbolic tangent sigmoid. In this study, the activation functions of the output and hidden neurons were set as linear and hyperbolic tangent sigmoid, respectively

$$\varphi(net_j) = net_j \tag{16}$$

$$\varphi(net_j) = \frac{2}{1+e^{-2net_j}} - 1 \tag{17}$$

The first is the identity function, and the latter takes the *net* values in the range $(-\infty, \infty)$ and converts it into an output in the interval $(-1, 1)$.

The neural network toolbox provided by MATLAB-2016a was used to develop the model. A multilayer perceptron (MLP) network with one hidden layer was used to form the ANN architecture. Adjusting the weight to ensure the desired output, based on experimental data, is defined as the training process. Given the acceptable performance in solving problems related to concrete materials[78,79] the back-propagation learning algorithm[80] was employed to train the system. This learning process consists of two main steps:

1. A forward flow of the input signal from the input layer toward the output layer and a calculation of error based on the comparison between the network's output and the target value—that is, experimental data. The cost function (error) to be minimized (with respect to the ANN weights $\boldsymbol{w}$) is given by

$$J(\boldsymbol{w}) = \frac{1}{2N}\sum_{i=1}^{N}\left[\boldsymbol{y}_i - \hat{\boldsymbol{y}}_i\right]^2 \tag{18}$$

where $\hat{\boldsymbol{y}}_i = f(x_i, \boldsymbol{w})$ is the output of the neural network when using a training set composed of N samples of {input, output} pairs: $\mathcal{T} = \{\boldsymbol{x}_i, \boldsymbol{y}_i\}_{i=1}^{N}$.

2. Backward propagation of the error signal and an adjustment of all the neurons' weights to minimize the error according to the generalized delta rule

$$\boldsymbol{w}^{new} = \boldsymbol{w}^{old} + \Delta\boldsymbol{w}^{old} \tag{19}$$

In this work, the optimization method of Levenberg-Marquardt backpropagation (LMBP) was used to train the MLP[81,82] because it is well-known to be effective[83-85]

$$\Delta\boldsymbol{w} = [\boldsymbol{H} + \mu\boldsymbol{I}]^{-1}\boldsymbol{g} \tag{20}$$

$$\boldsymbol{g} = \nabla_w J(\boldsymbol{w}) = \frac{\partial J(\boldsymbol{w})}{\partial \boldsymbol{w}} \tag{21}$$

Table 3—ANN parameters when performing hidden layer parameter sweep analysis

	Parameter value per scenario (GA)				
	Number of parameters				
Parameter description	13	18	15	21	Default parameters
Training method	LMBP	LMBP	LM P	LMBP	LMBP
Cost function	MSE	MSE	MSE	MSE	MSE
Number of hidden neurons (N)	7	7	28	16	(11, 8, 10, 8)
Maximum number of validation checks (V)	9	9	7	6	10
Initial regularizing parameter (μ)	0.7	0.14	0.03	0.03	0.001
Regularizing parameter decrease ratio (μ^-)	0.2	0.26	0.50	0.14	0.1
Regularizing param. increase ratio (μ^+)	2.4	2.8	2.70	5.10	10
Maximum regularizing parameter (μ_{max})	10^{10}	10^{10}	10^{10}	10^{10}	10^{10}

$$\boldsymbol{H} = \nabla^2_{w} J(\boldsymbol{w}) = \frac{\partial^2 J(\boldsymbol{w})}{\partial \boldsymbol{w}^2} \tag{22}$$

where μ is a regularizing parameter; $\boldsymbol{g}$ and $\boldsymbol{H}$ are the gradient and Hessian of the cost function $J(\boldsymbol{w})$; and $\boldsymbol{I}$ is the identity matrix. If the cost function increases, the regularizing parameter is increased by a factor of μ^+; otherwise, it is decreased by μ^- and the generalized delta rule is applied to update the weights.

Early stopping criterion based on consecutive validation set error checks was used to avoid overfitting the training data and to allow a better generalization performance of the MLP for previously unseen data. Additionally, each input parameter was scaled to the range (–1, 1).

In this study, a genetic algorithm (GA)[86] with integer representation was used to tune the internal parameters of the MLP, specifically, the number of hidden neurons, the maximum number of validation checks, the initial regularizing parameter value, and its increase and decrease ratios.

A total of 436 data samples, corresponding to 90% of the data available in the developed database, were randomly selected for training the neural network. The 43 data series obtained from laboratory investigations (discussed in the aforementioned "Laboratory investigation" section) were used for model validation. The remaining 10% of the data from the database were used for testing the selected model.

The GA optimization was carried out using a population of 100 individuals for 100 generations. To measure the performance consistency of a given ANN parameter configuration, the fitness function of the GA was defined as the median of the validation mean square error (MSE) of a given parameter configuration after the realization of 30 trials, each of which with random weight initialization (to address the local optima issues common to these types of neural networks). The ANN parameters optimized using GA included the number of hidden neurons (N) within the range of [1, 30] and 30 grid points, the maximum number of validation checks (V) within the range of [3, 10] and eight grid points, the initial regularizing parameter (μ) within the range of [0.001, 1] and 1000 grid points, the regularizing parameter decrease ratio (μ^-) within the range of [0.1, 0.8] and 100 grid points, and the regularizing parameter increase ratio (μ^+) within the range of [1.5, 10] and 100 grid points. These parameters were discretized using a grid of linearly and equally spaced points within their respective ranges from which the GA was used to evolve the best combination. The optimization toolbox provided by MATLAB-2016a was used to perform this parameter tuning. The following fixed parameters were considered during the GA optimization: LMBP training method and MSE cost function were used, respectively. The maximum training time was fixed at 1 second while the maximum number of epochs was 10^2. The performance goal was 0, with a minimum gradient of 10^{-7} and the maximum regularizing parameter (μ_{max}) of 10^3.

The GA was run 10 times and the solutions obtained were used in the next step of the model development, which consisted of running 1000 trials for each of the ANN parameter configurations and selecting the one with the best performance in terms of the validation set error. In case of a tie, the architecture with the best training error was selected. For fine-tuning purposes, an additional parameter sweep analysis of the number of hidden neurons was carried out by fixing the other parameters around values close to the solutions obtained by the GA. This setting of the number of neurons in the MLP's hidden layer is related to the approach discussed in Reference 79, in which the number of neurons is varied and the best architecture is selected. Finally, the same procedure was performed with an equal set of default parameters for all scenarios. The selected parameters are listed in Table 3.

The performance metrics—that is, regression results and MSE summarizing the correlations between the estimated values (neural network's output) and the experimental data (target values)—of all the ANNs after the parameter tuning process are listed in Table 4. For each case, the optimal ANN parameter configuration for the training, validation, and test subsets were incorporated as defined earlier to investigate the different subsets of features including 13, 15, 18, or 21 input parameters. Strong correlations were observed for the investigated models. The obtained correlation (R) values ranged from 0.71 to 0.95 for the training phase, 0.86 to 0.92 for the validation phase, and 0.74 to 0.89 for the testing phase. The MSE values ranged from 0.00140 to 0.00690 for the training, 0.00128 to 0.00218 for the validation, and 0.00359 to 0.00848 for the testing phases. The bolded values

Table 4—Summary of performance of various models

Scenario	*R*			MSE		
	Train.	Valid.	Test	Train.	Valid.	Test
After hidden layer parameter sweep analysis and using remaining parameter values close to GA solutions						
(I) 13 features	**0.9287***	0.8634	**0.8906**	**0.00187**	0.00218	**0.00359**
(II) 18 features	0.9389	**0.9193**	**0.8332**	0.00161	0.00196	**0.00571**
(III) 15 features	0.7098	**0.9123**	0.8092	0.00690	**0.00155**	0.00620
(IV) 21 features	**0.9396**	0.9086	0.8460	**0.00160**	0.00142	0.00511
After hidden neurons parameter sweep analysis using default parameters						
(I) 13 features†	0.9259	**0.8750**	0.8861	0.00194	**0.00193**	0.00382
(II) 18 features	**0.9472**	0.8959	0.7410	**0.00140**	**0.00159**	0.00848
(III) 15 features	**0.9298**	0.8794	**0.8846**	**0.00184**	0.00180	**0.00382**
(IV) 21 features	0.9138	**0.9175**	**0.8677**	0.00225	**0.00128**	**0.00424**

*Bold values indicate best performance across train, validation, and test sets.

†Selected model.

indicate best performance across train, validation, and test sets in Table 4.

RESULTS AND DISCUSSION

Model selection

The results presented in Table 4 suggest that the MLP is robust with respect to the parameter selection for this specific function approximation problem. Additionally, in terms of minimum MSE and the correlation coefficient (*R*), the prediction performances of the four models regarding their respective scenarios seem comparable. Therefore, based on Occam's razor[87]—that is, the principle of parsimony—the simplest model was selected: Scenario I with default parameters due to the smaller validation error. In other words, given the requirements for proper prediction are met, it is generally recommended to select regression models with a lower number of input parameters. It is also recommended to avoid dependent variables as input parameters to avoid multi-collinearity, unless it is proven that the incorporation of such features can enhance the model performance. Figure 3 presents the correlations between the neural network's predictions about the selected model and the experimental values obtained during training, validation, and testing along with their respective MSEs. Figure 4 depicts the MLP prediction and the experimental value of the R_{MOE} side by side for each sample. A reasonable match was obtained between the model predictions and the experimental values of R_{MOE}, especially considering that the training data consisted of a collection of samples from technical publications (with case-by-case variations in experimental procedures, instruments, and conditions) with missing values that still needed to be estimated; nevertheless, the ANN performs reasonably well in the validation (population of laboratory experiments) and in the test set. This fact indicates that the MLP is an adequate modeling tool for this estimation problem.

Case study

The model will be applicable for a wide range of applications as long as the input parameters are within the range of the database used for model development. Given the fact that transportation infrastructure is one of the main potential markets for RCA consumption, the selected model was employed to quantify the effect of RCA on MOE of concrete for rigid pavement construction. The test scenario involved investigating the rate of variation in the MOE of concrete prepared with 323 kg/m^3 (545 lb/yd^3) of cementitious materials and 0.40 *w*/*cm*. The simulated mixture was made with virgin coarse aggregate with 0.8% water absorption, 2730 kg/m^3 (170 lb/ft^3) specific gravity, and 28% LA abrasion mass loss. The range of the investigated RCA properties were water absorption of 1.8% to 8.5%, oven-dry specific gravity of 2100 to 2500 kg/m^3 (131 to 156 lb/ft^3) and a replacement rate of 0 to 100% (by mass) for the simulation according to Scenario I. It should be noted that the mixture design and material properties used for case study are well within the typical criteria for rigid pavement construction used by state departments of transportations.[88]

Figure 5 presents the effect of RCA water absorption and the replacement rate (% mass) on the extent of variation in the MOE based on the model investigated in Scenario I. In general, the results indicate a reduction in the MOE due to the use of RCA with higher water absorption. The rate of reduction in the MOE was limited to 10% when RCA with water absorption limited to 2.5% was used (even up to 100% replacement). The rate of reduction in the MOE was 10%, 15%, and 20% when 30%, 50%, and 100% RCA with water absorption of 4% was used in pavement concrete. The reduction rate was 15%, 20%, and 40% when 30%, 50%, and 100% RCA with water absorption of 6% was used.

Figure 6 presents the effect of RCA oven dry specific gravity on the rate of variation in the MOE at different replacement ratios (% mass). In general, a reduction in MOE was observed as a result of using RCA with a lower oven-dry specific gravity. However, the reduction in the MOE was limited to 10% when RCA with an oven-dry specific gravity higher than 2500 kg/m^3 (156 lb/ft^3) was used. The results presented in Fig. 6 indicate a respective 15%, 25%, and 45% reduction in the MOE when 30%, 50%, and 100% RCA with an oven-dry specific gravity of 2200 kg/m^3 (137 lb/ft^3) was used in pavement concrete. The rate of reduction in the MOE

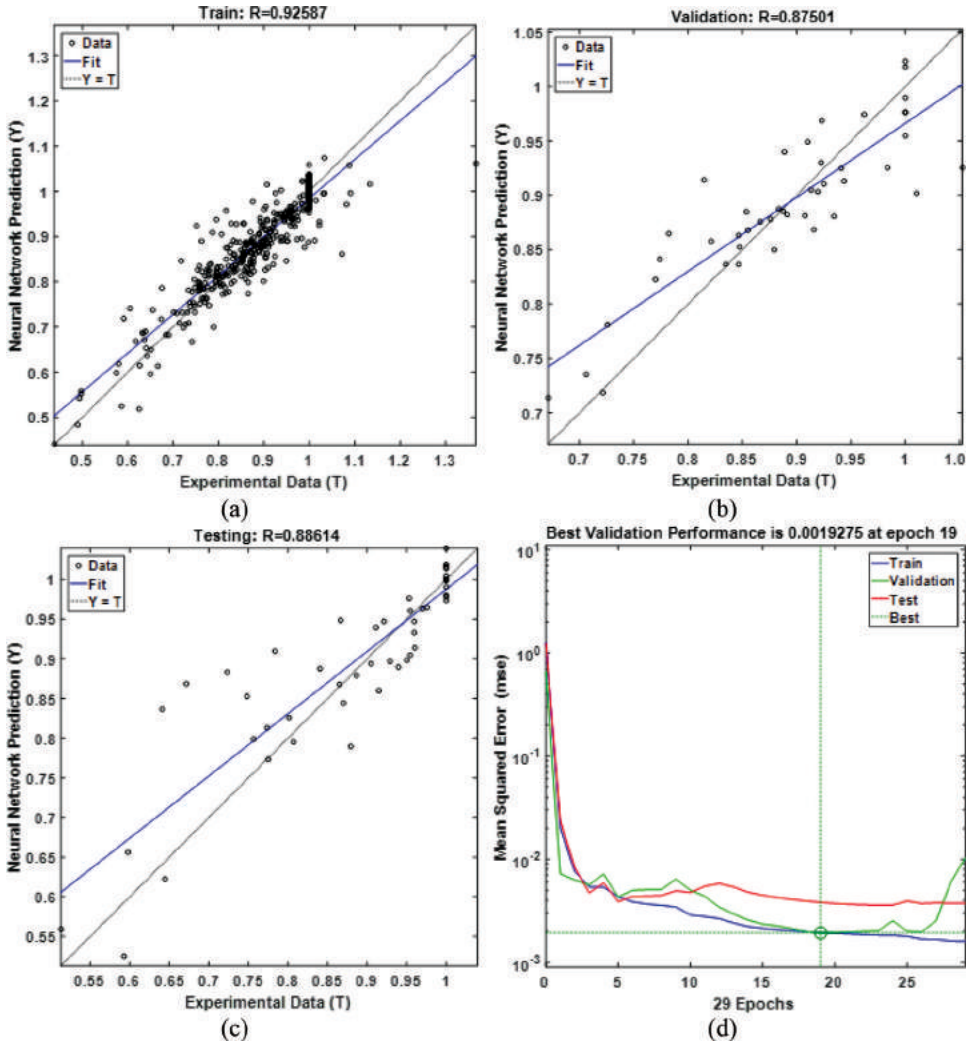

Fig. 3—ANN model performance with 13 input parameters (Scenario I). Correlation coefficient between experimental values and ANN predictions for: (a) training; (b) validation; and (c) testing is shown. MSE during training, validation, and testing is depicted in: (d) as function of training epochs (one epoch corresponds to an entire pass through the training data samples).

was respectively 15%, 20%, and 30% when 30%, 50%, and 100% RCA with an oven-dry specific gravity of 2300 kg/m^3 (143.6 lb/ft^3) was used. The results presented in Fig. 5 and 6 also revealed that the use of 30% and 50% RCA can lead to a respective reduction of up to 20% and 30% in the MOE of pavement concrete when low-quality RCA with an oven-dry specific gravity of 2100 kg/m^3 (131 lb/ft^3) and water absorption as high as 8.5% is used.

SUMMARY AND CONCLUSIONS

A database was developed to investigate the effect of coarse RCA on the MOE of concrete. Over 480 data series were extracted from 52 technical papers to form the database. The database includes key physical properties of the coarse RCA and mixture proportioning of the concrete. ANN was employed for the analysis of the database. Four different input scenarios were considered to investigate different combinations of the input parameters. The scenarios included concrete mixture design parameters and key properties of the virgin and recycled aggregate. Data obtained from testing 43 concrete mixtures were incorporated to validate the developed models. Based on the results presented herein, the following conclusions can be drawn:

- A multilayer perceptron network and Levenberg-Marquardt backward propagation learning algorithm were successfully used to develop and optimize the ANN architecture with one hidden layer for estimating the variations in the MOE of concrete made with RCA.
- The validation results indicated that there is a strong correlation between the experimental target values and the data obtained through the simulation, with a coefficient of correlation ranging from 0.86 to 0.92 and a mean square error limited to 0.002 for the selected model. The results obtained from testing the model with independent data from the database indicated acceptable performance, with a coefficient of correlation ranging from 0.74 to 0.89 for the investigated models.
- The data obtained from the analysis indicated that, in addition to the mixture design parameters and the RCA replacement rate, the oven-dry specific gravity and/or water absorption of RCA can be used for quantifying the effect of coarse RCA on concrete MOE.

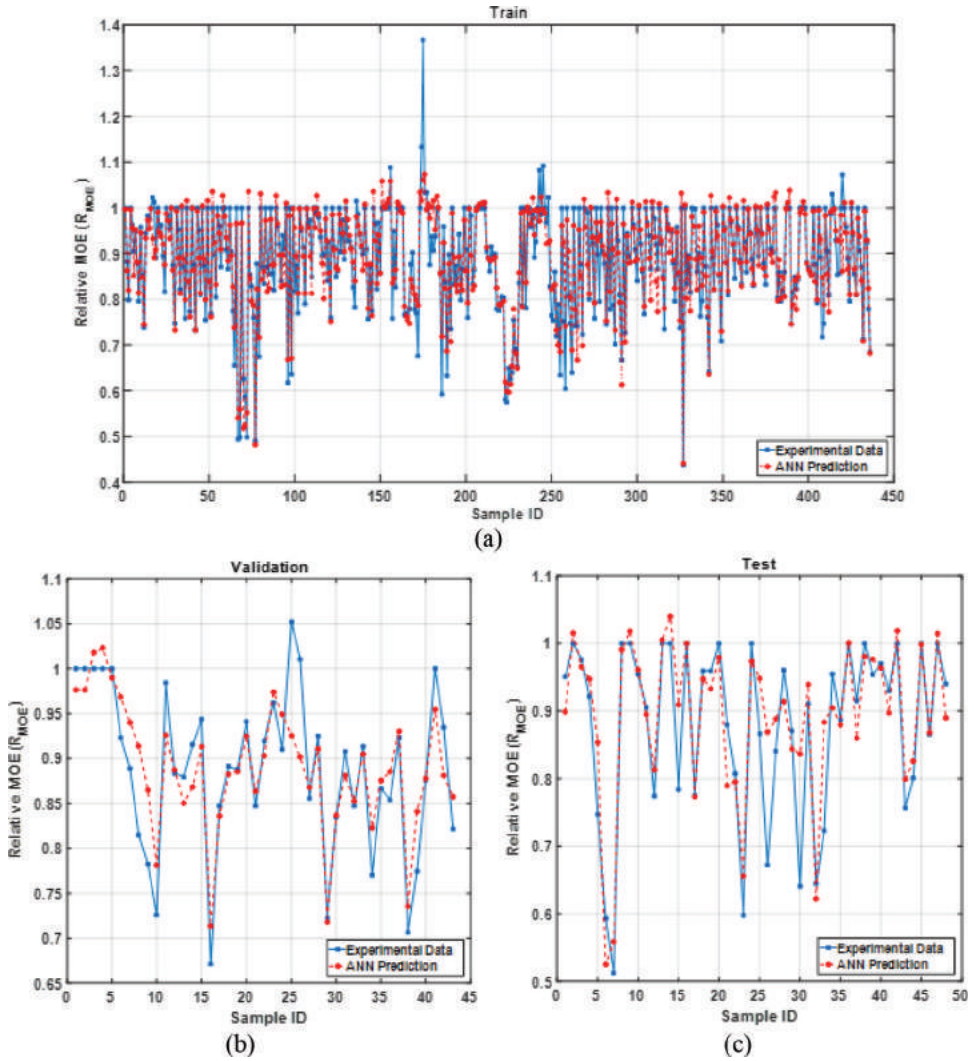

Fig. 4—ANN model prediction (Scenario I with default parameters) and experimental data for: (a) training; (b) validation; and (c) testing versus their respective input indexes (Sample ID).

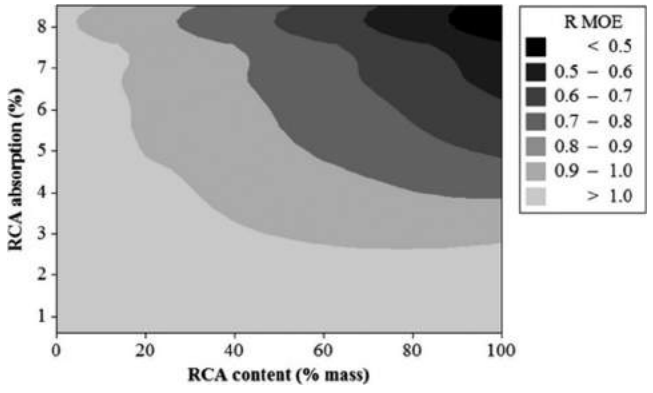

Fig. 5—Effect of RCA water absorption on MOE of concrete designated for rigid pavement construction, Scenario I.

- The results obtained through the case study indicate that the reduction in the MOE of pavement concrete can be limited to 10% when coarse RCA with water absorption lower than 2.5% or an oven-dry specific gravity higher than 2500 kg/m^3 (156 lb/ft^3) is used, even at the full replacement rate.

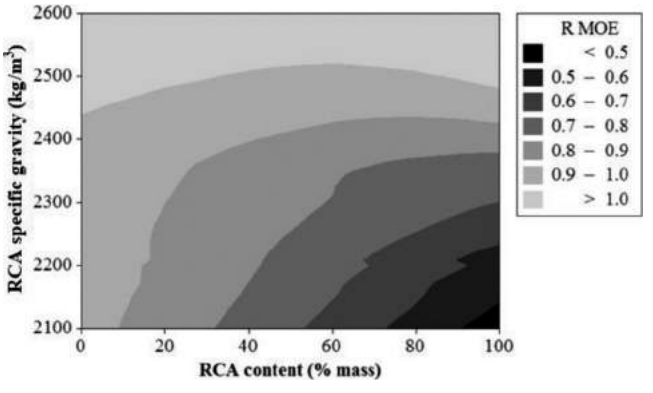

Fig. 6—Effect of RCA oven-dry specific gravity on MOE of concrete designated for rigid pavement construction, Scenario I.

- The use of 30% and 50% RCA can lead to a respective reduction of up to 20% and 30% in the MOE of pavement concrete when low-quality RCA with an oven dry specific gravity of 2100 kg/m^3 (131 lb/ft^3) and water absorption as high as 8.5% is used.

AUTHOR BIOS

Seyedhamed Sadati *is an Assistant Scientist at Iowa State University, Ames, IA. His research interests include durability of concrete and cement-based materials, sustainability, and properties of concrete made with recycled aggregate.*

Leonardo Enzo Brito da Silva *is a PhD Candidate in computer engineering at the Applied Computational Intelligence Laboratory, Electrical and Computer Engineering Department, Missouri S&T, Rolla, MO. His research interests include machine learning, neural networks, and information theory.*

Donald C. Wunsch II *is the Mary Finley Missouri Distinguished Professor of Computer Engineering and Director of the Applied Computational Intelligence Laboratory at Missouri S&T. His research interests include unsupervised, reinforcement, and mixed-modality learning; and applications to social computing, games, bioinformatics, energy, and defense.*

Kamal H. Khayat, *FACI, is Professor of civil engineering at Missouri S&T. He is a member of ACI's Technical Activities Committee, the* ACI Materials Journal *Editorial Board, and ACI Committees 234, Silica Fume in Concrete; 236, Materials Science of Concrete; 237, Self-Consolidating Concrete; 238, Workability of Concrete; and 552, Cementitious Grouting. His research interests include self-consolidating concrete, high-performance concrete, rheology of cement-based materials, and concrete repair.*

ACKNOWLEDGMENTS

The authors gratefully acknowledge the financial support provided by the Missouri Department of Transportation and the RE-CAST Tier 1 University Transportation Center at Missouri S&T. Support from the National Science Foundation, the Missouri University of Science and Technology Intelligent Systems Center, and the Mary K. Finley Endowment is also gratefully acknowledged. The second author was supported by the CAPES Foundation, Ministry of Education of Brazil, under Grant Number BEX 13494/13-9. This research was sponsored by the Army Research Laboratory (ARL), and it was accomplished under Cooperative Agreement Number W911NF-18-2-0260. The views and conclusions contained in this document are those of the authors and should not be interpreted as representing the official policies, either expressed or implied, of the Army Research Laboratory or the U.S. Government. The U.S. Government is authorized to reproduce and distribute reprints for Government purposes notwithstanding any copyright notation herein.

REFERENCES

1. United States Environmental Protection Agency, "RCRA in Focus: Construction, Demolition, and Renovation," Washington, DC, 2004, https://www.epa.gov/hwgenerators/resource-conservation-and-recovery-act-rcra-focus-hazardous-waste-generator-guidance. (last accessed Jan. 29, 2019)

2. United States Environmental Protection Agency, "Advancing Sustainable Materials Management: 2013 Fact Sheet," Washington, DC, 2015, https://www.epa.gov/sites/production/files/2015-09/documents/2013_advncng_smm_fs.pdf. (last accessed Jan. 29, 2019)

3. United States Environmental Protection Agency, "Advancing Sustainable Materials Management: 2014 Fact Sheet," Washington, DC, 2016, https://www.epa.gov/sites/production/files/2016-11/documents/2014_smmfactsheet_508.pdf. (last accessed Jan. 29, 2019)

4. Gonzalez, G. P., and Moo-Young, H. K., "Transportation Applications of Recycled Concrete Aggregate," *FHWA State of the Practice National Review*, Federal Highway Administration, Washington, DC, 2004, 47 pp.

5. National Academies of Sciences, Engineering, and Medicine, "Recycled Materials and Byproducts in Highway Applications—Reclaimed Asphalt Pavement, Recycled Concrete Aggregate, and Construction Demolition Waste," V. 6, *The National Academies Press*, Washington, DC, 2013. /https://doi.org/10.17226/22547.10.17226/22547

6. Monteiro, P., *Concrete: Microstructure, Properties, and Materials*, McGraw-Hill Publishing, New York, 2006.

7. Knaack, A. M., and Kurama, Y. C., "Behavior of Reinforced Concrete Beams with Recycled Concrete Coarse Aggregates," *Journal of Structural Engineering*, ASCE, V. 141, No. 3, 2015, p. B4014009 doi: 10.1061/(ASCE)ST.1943-541X.0001118

8. Fonseca, N.; De Brito, J.; and Evangelista, L., "The Influence of Curing Conditions on the Mechanical Performance of Concrete Made with Recycled Concrete Waste," *Cement and Concrete Composites*, V. 33, No. 6, 2011, pp. 637-643. doi: 10.1016/j.cemconcomp.2011.04.002

9. Vieira, J. P. B.; Correia, J. R.; and De Brito, J., "Post-Fire Residual Mechanical Properties of Concrete Made with Recycled Concrete Coarse Aggregates," *Cement and Concrete Research*, V. 41, No. 5, 2011, pp. 533-541. doi: 10.1016/j.cemconres.2011.02.002

10. Eurocode 2:1992, "European Standard EN 1992-1-1: Eurocode 2: Design of Concrete Structures: Part 1-1: General Rules and Rules for Buildings," Stage 51 Draft, Comite Europeen de Normalisation, Brussels, Belgium, Dec. 2003.

11. Japan Society of Civil Engineers, "Standard Specification for Concrete Structure (JSCE No. 15)," Tokyo, Japan, 2007.

12. ACI Committee 318, "Building Code Requirements for Structural Concrete (ACI 318-14) and Commentary (ACI 318R-14)," American Concrete Institute, Farmington Hills, MI, 2014, 520 pp.

13. Behnood, A.; Olek, J.; and Glinicki, M. A., "Predicting Modulus Elasticity of Recycled Aggregate Concrete Using M5′ Model Tree Algorithm," *Construction and Building Materials*, V. 94, 2015, pp. 137-147. doi: 10.1016/j.conbuildmat.2015.06.055

14. Ravindrarajah, R. S., and Tam, C. T., "Properties of Concrete Made with Crushed Concrete as Coarse Aggregate," *Magazine of Concrete Research*, V. 37, No. 130, 1985, pp. 29-38. doi: 10.1680/macr.1985.37.130.29

15. Dhir, R. K.; Limbachiya, M. C.; and Leelawat, T., "Suitability of Recycled Aggregate for Use in BS 5328 Designated Mixes," *Proceedings of the Institution of Civil Engineers. Structures and Buildings*, V. 134, No. 3, 1999, pp. 257-274. doi: 10.1680/istbu.1999.31568

16. Dillmann, R., "Concrete with Recycled Concrete Aggregate," *Proceedings of International Symposium on Sustainable Construction: Use of Recycled Concrete Aggregate*, Dundee, UK, 1998, pp. 239-253.

17. Mellmann, G., "Processed Concrete Rubble for the Reuse as Aggregate," *Proceedings of the International Seminar on Exploiting Waste in Concrete*, Dundee, UK, 1999, pp. 171-178.

18. Kakizaki, M.; Harada, M.; Soshiroda, T.; Kubota, S.; Ikeda, T.; and Kasai, Y., "Strength and Elastic Modulus of Recycled Aggregate Concrete," *Proceedings of the Second International RILEM Symposium on Demolition and Reuse of Concrete and Masonry*, Tokyo, Japan, 1988, pp. 565-574.

19. Zilch, K., and Roos, F., "An Equation to Estimate the Modulus of Elasticity of Concrete with Recycled Aggregates," *Civil Engineering (New York, N.Y.)*, V. 76, No. 4, 2001, pp. 187-191. (only available in German)

20. Corinaldesi, V., "Mechanical and Elastic Behaviour of Concretes Made of Recycled-Concrete Coarse Aggregates," *Construction and Building Materials*, V. 24, No. 9, 2010, pp. 1616-1620. doi: 10.1016/j.conbuildmat.2010.02.031

21. Xiao, J. Z.; Li, J. B.; and Zhang, C., "On Relationships between the Mechanical Properties of Recycled Aggregate Concrete: An Overview," *Materials and Structures*, V. 39, No. 6, 2007, pp. 655-664. doi: 10.1617/s11527-006-9093-0

22. Deng, F.; He, Y.; Zhou, S.; Yu, Y.; Cheng, H.; and Wu, X., "Compressive Strength Prediction of Recycled Concrete Based on Deep Learning," *Construction and Building Materials*, V. 175, 2018, pp. 562-569. doi: 10.1016/j.conbuildmat.2018.04.169

23. Naderpour, H.; Rafiean, A. H.; and Fakharian, P., "Compressive Strength Prediction of Environmentally Friendly Concrete Using Artificial Neural Networks," *Journal of Building Engineering*, V. 16, 2018, pp. 213-219. doi: 10.1016/j.jobe.2018.01.007

24. Adams, M. P.; Fu, T.; Cabrera, A. G.; Morales, M.; Ideker, J. H.; and Isgor, O. B., "Cracking Susceptibility of Concrete Made with Coarse Recycled Concrete Aggregates," *Construction and Building Materials*, V. 102, 2016, pp. 802-810. doi: 10.1016/j.conbuildmat.2015.11.022

25. Akbarnezhad, A.; Ong, K. C. G.; Zhang, M. H.; Tam, C. T.; and Foo, T. W. J., "Microwave-Assisted Beneficiation of Recycled Concrete Aggregates," *Construction and Building Materials*, V. 25, No. 8, 2011, pp. 3469-3479. doi: 10.1016/j.conbuildmat.2011.03.038

26. Andreu, G., and Miren, E., "Experimental Analysis of Properties of High Performance Recycled Aggregate Concrete," *Construction and Building Materials*, V. 52, 2014, pp. 227-235. doi: 10.1016/j.conbuildmat.2013.11.054

27. Arezoumandi, M.; Drury, J.; Volz, J. S.; and Khayat, K. H., "Effect of Recycled Concrete Aggregate Replacement Level on Shear Strength of Reinforced Concrete Beams," *ACI Materials Journal*, V. 112, No. 4, July-Aug. 2015, pp. 559-568. doi: 10.14359/51687766

28. Bravo, M.; de Brito, J.; Pontes, J.; and Evangelista, L., "Mechanical Performance of Concrete Made with Aggregates from Construction and Demolition Waste Recycling Plants," *Journal of Cleaner Production*, V. 99, 2015, pp. 59-74. doi: 10.1016/j.jclepro.2015.03.012

29. Cachim, P. B., "Mechanical Properties of Brick Aggregate Concrete," *Construction and Building Materials*, V. 23, No. 3, 2009, pp. 1292-1297. doi: 10.1016/j.conbuildmat.2008.07.023

30. Casuccio, M.; Torrijos, M. C.; Giaccio, G.; and Zerbino, R., "Failure Mechanism of Recycled Aggregate Concrete," *Construction and Building Materials*, V. 22, No. 7, 2008, pp. 1500-1506. doi: 10.1016/j.conbuildmat.2007.03.032

31. Choi, W. C., and Yun, H. D., "Compressive Behavior of Reinforced Concrete Columns with Recycled Aggregate under Uniaxial Loading," *Engineering Structures*, V. 41, 2012, pp. 285-293. doi: 10.1016/j.engstruct.2012.03.037

32. Cui, H. Z.; Shi, X.; Memon, S. A.; Xing, F.; and Tang, W., "Experimental Study on the Influence of Water Absorption of Recycled Coarse Aggregates on Properties of the Resulting Concretes," *Journal of Materials in Civil Engineering*, ASCE, V. 27, No. 4, 2015, p. 04014138 doi: 10.1061/(ASCE)MT.1943-5533.0001086

33. Dapena, E.; Alaejos, P.; Lobet, A.; and Pérez, D., "Effect of Recycled Sand Content on Characteristics of Mortars and Concretes," *Journal of Materials in Civil Engineering*, ASCE, V. 23, No. 4, 2011, pp. 414-422. doi: 10.1061/(ASCE)MT.1943-5533.0000183

34. De Juan, M. S., and Gutiérrez, P. A., "Influence of Recycled Aggregate Quality on Concrete Properties," Conference on Use of Recycled Materials in Building and Structures, 2004, pp. 9-11.

35. Debieb, F.; Courard, L.; Kenai, S.; and Degeimbre, R., "Mechanical and Durability Properties of Concrete Using Contaminated Recycled Aggregates," *Cement and Concrete Composites*, V. 32, No. 6, 2010, pp. 421-426. doi: 10.1016/j.cemconcomp.2010.03.004

36. Dilbas, H.; Şimşek, M.; and Çakır, Ö., "An Investigation on Mechanical and Physical Properties of Recycled Aggregate Concrete (RAC) with and without Silica Fume," *Construction and Building Materials*, V. 61, 2014, pp. 50-59. doi: 10.1016/j.conbuildmat.2014.02.057

37. Dong, J. F.; Wang, Q. Y.; and Guan, Z. W., "Structural Behaviour of Recycled Aggregate Concrete Filled Steel Tube Columns Strengthened by CFRP," *Engineering Structures*, V. 48, 2013, pp. 532-542. doi: 10.1016/j.engstruct.2012.11.006

38. Duan, Z. H., and Poon, C. S., "Properties of Recycled Aggregate Concrete Made with Recycled Aggregates with Different Amounts of Old Adhered Mortars," *Materials & Design*, V. 58, 2014, pp. 19-29. doi: 10.1016/j.matdes.2014.01.044

39. Etxeberria, M.; Vázquez, E.; Marí, A.; and Barra, M., "Influence of Amount of Recycled Coarse Aggregates and Production Process on Properties of Recycled Aggregate Concrete," *Cement and Concrete Research*, V. 37, No. 5, 2007, pp. 735-742. doi: 10.1016/j.cemconres.2007.02.002

40. Geng, Y.; Wang, Y.; and Chen, J., "Time-Dependent Behaviour of Steel Tubular Columns Filled with Recycled Coarse Aggregate Concrete," *Journal of Constructional Steel Research*, V. 122, 2016, pp. 455-468. doi: 10.1016/j.jcsr.2016.04.009

41. Gómez-Soberón, J. M., "Porosity of Recycled Concrete with Substitution of Recycled Concrete Aggregate: An Experimental Study," *Cement and Concrete Research*, V. 32, No. 8, 2002, pp. 1301-1311. doi: 10.1016/S0008-8846(02)00795-0

42. Gonzalez-Corominas, A., and Etxeberria, M., "Properties of High Performance Concrete Made with Recycled Fine Ceramic and Coarse Mixed Aggregates," *Construction and Building Materials*, V. 68, 2014, pp. 618-626. doi: 10.1016/j.conbuildmat.2014.07.016

43. Gonzalez-Corominas, A., and Etxeberria, M., "Effects of Using Recycled Concrete Aggregates on the Shrinkage of High Performance Concrete," *Construction and Building Materials*, V. 115, 2016, pp. 32-41. doi: 10.1016/j.conbuildmat.2016.04.031

44. Gonzalez-Corominas, A.; Etxeberria, M.; and Poon, C. S., "Influence of Steam Curing on the Pore Structures and Mechanical Properties of Fly-Ash High Performance Concrete Prepared with Recycled Aggregates," *Cement and Concrete Composites*, V. 71, 2016, pp. 77-84. doi: 10.1016/j.cemconcomp.2016.05.010

45. González-Fonteboa, B., and Martínez-Abella, F., "Recycled Aggregates Concrete: Aggregate and Mix Properties," *Materiales de Construcción*, V. 55, No. 279, 2005, pp. 53-66.

46. González-Fonteboa, B.; Martínez-Abella, F.; Eiras-López, J.; and Seara-Paz, S., "Effect of Recycled Coarse Aggregate on Damage of Recycled Concrete," *Materials and Structures*, V. 44, No. 10, 2011, pp. 1759-1771. doi: 10.1617/s11527-011-9736-7

47. Henry, M.; Pardo, G.; Nishimura, T.; and Kato, Y., "Balancing Durability and Environmental Impact in Concrete Combining Low-Grade Recycled Aggregates and Mineral Admixtures," *Resources, Conservation and Recycling*, V. 55, No. 11, 2011, pp. 1060-1069. doi: 10.1016/j.resconrec.2011.05.020

48. Ignjatović, I. S.; Marinković, S. B.; Mišković, Z. M.; and Savić, A. R., "Flexural Behavior of Reinforced Recycled Aggregate Concrete Beams under Short-Term Loading," *Materials and Structures*, V. 46, No. 6, 2013, pp. 1045-1059. doi: 10.1617/s11527-012-9952-9

49. Kang, T. H.; Kim, W.; Kwak, Y. K.; and Hong, S. G., "Flexural Testing of Reinforced Concrete Beams with Recycled Concrete Aggregates," *ACI Structural Journal*, V. 111, No. 3, May-June 2014, pp. 607-615. doi: 10.14359/51686622

50. Katz, A., "Properties of Concrete Made with Recycled Aggregate from Partially Hydrated Old Concrete," *Cement and Concrete Research*, V. 33, No. 5, 2003, pp. 703-711. doi: 10.1016/S0008-8846(02)01033-5

51. Kou, S. C., and Poon, C. S., "Long-Term Mechanical and Durability Properties of Recycled Aggregate Concrete Prepared with the Incorporation of Fly Ash," *Cement and Concrete Composites*, V. 37, 2013, pp. 12-19. doi: 10.1016/j.cemconcomp.2012.12.011

52. Kou, S. C.; Poon, C. S.; and Chan, D., "Influence of Fly Ash as Cement Replacement on the Properties of Recycled Aggregate Concrete," *Journal of Materials in Civil Engineering*, ASCE, V. 19, No. 9, 2007, pp. 709-717. doi: 10.1061/(ASCE)0899-1561(2007)19:9(709)

53. Kou, S. C.; Poon, C. S.; and Chan, D., "Influence of Fly Ash as a Cement Addition on the Hardened Properties of Recycled Aggregate Concrete," *Materials and Structures*, V. 41, No. 7, 2008, pp. 1191-1201. doi: 10.1617/s11527-007-9317-y

54. Kou, S. C.; Poon, C. S.; and Wan, H. W., "Properties of Concrete Prepared with Low-Grade Recycled Aggregates," *Construction and Building Materials*, V. 36, 2012, pp. 881-889. doi: 10.1016/j.conbuildmat.2012.06.060

55. Koulouris, A.; Limbachiya, M. C.; Fried, A. N.; and Roberts, J. J., "Use of Recycled Aggregate in Concrete Application: Case studies." *Proceedings of the International Conference on Sustainable Waste Management and Recycling: Challenges and Opportunities*, Thomas Telford, London, UK, pp. 245-257.

56. Laserna, S., and Montero, J., "Influence of Natural aggregates Typology on Recycled Concrete Strength Properties," *Construction and Building Materials*, V. 115, 2016, pp. 78-86. doi: 10.1016/j.conbuildmat.2016.04.037

57. Limbachiya, M.; Meddah, M. S.; and Ouchagour, Y., "Performance of Portland/Silica Fume Cement Concrete Produced with Recycled Concrete Aggregate," *ACI Materials Journal*, V. 109, No. 1, Jan.-Feb. 2012, pp. 91-100.

58. Pedro, D.; De Brito, J.; and Evangelista, L., "Influence of the Use of Recycled Concrete Aggregates from Different Sources on Structural Concrete," *Construction and Building Materials*, V. 71, 2014, pp. 141-151. doi: 10.1016/j.conbuildmat.2014.08.030

59. Pedro, D.; De Brito, J.; and Evangelista, L., "Performance of Concrete Made with Aggregates Recycled from Precasting Industry Waste: Influence of the Crushing Process," *Materials and Structures*, V. 48, No. 12, 2015, pp. 3965-3978. doi: 10.1617/s11527-014-0456-7

60. Rahal, K., "Mechanical Properties of Concrete with Recycled Coarse Aggregate," *Building and Environment*, V. 42, No. 1, 2007, pp. 407-415. doi: 10.1016/j.buildenv.2005.07.033

61. Rao, M. C.; Bhattacharyya, S. K.; and Barai, S. V., "Influence of Field Recycled Coarse Aggregate on Properties of Concrete," *Materials and Structures*, V. 44, No. 1, 2011, pp. 205-220. doi: 10.1617/s11527-010-9620-x

62. Folino, P., and Xargay, H., "Recycled Aggregate Concrete—Mechanical Behavior under Iniaxial and Triaxial Compression," *Construction and Building Materials*, V. 56, 2014, pp. 21-31. doi: 10.1016/j.conbuildmat.2014.01.073

63. Salem, R. M.; Burdette, E. G.; and Jackson, N. M., "Resistance to Freezing and Thawing of Recycled Aggregate Concrete," *ACI Materials Journal*, V. 100, No. 3, May-June 2003, pp. 216-221.

64. Schubert, S.; Hoffmann, C.; Leemann, A.; Moser, K.; and Motavalli, M., "Recycled Aggregate Concrete: Experimental Shear Resistance of Slabs without Shear Reinforcement," *Engineering Structures*, V. 41, 2012, pp. 490-497. doi: 10.1016/j.engstruct.2012.04.006

65. Seara-Paz, S.; González-Fonteboa, B.; Martínez-Abella, F.; and González-Taboada, I., "Time-Dependent Behaviour of Structural Concrete Made with Recycled Coarse Aggregates. Creep and Shrinkage," *Construction and Building Materials*, V. 122, 2016, pp. 95-109. doi: 10.1016/j.conbuildmat.2016.06.050

66. Thomas, C.; Setién, J.; Polanco, J.; Alaejos, P.; and De Juan, M. S., "Durability of Recycled Aggregate Concrete," *Construction and Building Materials*, V. 40, 2013, pp. 1054-1065. doi: 10.1016/j.conbuildmat.2012.11.106

67. Wang, W. L.; Kou, S. C.; and Xing, F., "Deformation Properties and Direct Shear of Medium Strength Concrete Prepared with 100% Recycled Coarse Aggregates," *Construction and Building Materials*, V. 48, 2013, pp. 187-193. doi: 10.1016/j.conbuildmat.2013.06.065

68. Xiao, J.; Li, J.; and Zhang, C., "Mechanical Properties of Recycled Aggregate Concrete under Uniaxial Loading," *Cement and Concrete Research*, V. 35, No. 6, 2005, pp. 1187-1194. doi: 10.1016/j.cemconres.2004.09.020

69. Yang, K. H.; Chung, H. S.; and Ashour, A. F., "Influence of Type and Replacement Level of Recycled Aggregates on Concrete Properties," *ACI Materials Journal*, V. 105, No. 3, May-June 2008, pp. 289-296.

70. Zega, C. J., and Di Maio, A. A., "Recycled Concretes Made with Waste Ready-Mix Concrete as Coarse Aggregate," *Journal of Materials in Civil Engineering*, ASCE, V. 23, No. 3, 2011, pp. 281-286. doi: 10.1061/(ASCE)MT.1943-5533.0000165

71. Omary, S.; Ghorbel, E.; and Wardeh, G., "Relationships between Recycled Concrete Aggregates Characteristics and Recycled Aggregates Concretes Properties," *Construction and Building Materials*, V. 108, 2016, pp. 163-174. doi: 10.1016/j.conbuildmat.2016.01.042

72. Khayat, K. H., and Sadati, S., "High-Volume Recycled Materials for Sustainable Pavement Construction, Final *Report* No. crm17-006, Missouri Department of Transportation, Jefferson City, MO, 2016.

73. González-Taboada, I.; González-Fonteboa, B.; Martínez-Abella, F.; and Carro-López, D., "Study of Recycled Concrete Aggregate Quality and its Relationship with Recycled Concrete Compressive Strength Using Database Analysis," *Materiales de Construcción*, V. 66, No. 323, 2016, pp. 1-18.

74. ASTM C143/C143M-15, "Standard Test Method for Slump of Hydraulic-Cement Concrete," ASTM International, West Conshohocken, PA, 2015, 4 pp.

75. ASTM C231/C231-14, "Standard Test Method for Air Content of Freshly Mixed Concrete by the Pressure Method," ASTM International, West Conshohocken, PA, 2014, 9 pp.

76. ASTM C39/C39M-01, "Standard Test Method for Compressive Strength of Cylindrical Concrete Specimens," ASTM International, West Conshohocken, PA, 2001, 5 pp.

77. ASTM C469/C469M-10, "Standard Test Method for Static Modulus of Elasticity and Poisson's Ratio of Concrete in Compression," ASTM International, West Conshohocken, PA, 2010, 5 pp.

78. Duan, Z.; Poon, C. S.; and Xiao, J., "Using Artificial Neural Networks to Assess the Applicability of Recycled Aggregate Classification by Different Specifications," *Materials and Structures*, V. 50, No. 2, 2017, pp. 107-116. doi: 10.1617/s11527-016-0972-8

79. Ghafari, E.; Bandarabadi, M.; Costa, H.; and Júlio, E., "Prediction of Fresh and Hardened State Properties of UHPC: Comparative Study of Statistical Mixture Design and an Artificial Neural Network Model," *Journal of Materials in Civil Engineering*, ASCE, V. 27, No. 11, 2015, p. 04015017 doi: 10.1061/(ASCE)MT.1943-5533.0001270

80. Werbos, P. J., *The Roots of Backpropagation: From Ordered Derivatives to Neural Networks and Political Forecasting*, Wiley Interscience, 1994, 319 pp.

81. Levenberg, K., "A Method for the Solution of Certain Non-linear Problems in Least Squares," *Quarterly of Applied Mathematics*, V. 2, No. 2, 1944, pp. 164-168. doi: 10.1090/qam/10666

82. Marquardt, D. W., "An Algorithm for Least-Squares Estimation of Nonlinear Parameters," *Journal of the Society for Industrial and Applied Mathematics*, V. 11, No. 2, 1963, pp. 431-441. doi: 10.1137/0111030

83. Hagan, M. T., and Menhaj, M. B., "Training Feedforward Networks with the Marquardt Algorithm," *IEEE Transactions on Neural Networks*, V. 5, No. 6, 1994, pp. 989-993. doi: 10.1109/72.329697

84. Fu, X.; Li, S.; Fairbank, M.; Wunsch, D. C. II; and Alonso, E., "Training Recurrent Neural Networks with the Levenberg–Marquardt Algorithm for Optimal Control of a Grid-Connected Converter," *IEEE Transactions on Neural Networks and Learning Systems*, V. 26, No. 9, 2015, pp. 1900-1912. doi: 10.1109/TNNLS.2014.2361267

85. Haykin, S., *Neural Networks and Learning Machines*, Pearson Education, Upper Saddle River, NJ, 2009.

86. Eiben, A. E., and Smith, J. E., *Introduction to Evolutionary Computing*, Springer-Verlag, Berlin Heidelberg, 2007.

87. Duda, R. O.; Hart, P. E.; and Stork, D. G., *Pattern Classification*, second edition, Wiley, Hoboken, NJ, 2000.

88. Sadati, S., and Khayat, K. H., "Field Performance of Concrete Pavement Incorporating Recycled Concrete Aggregate," *Construction and Building Materials*, V. 126, 2016, pp. 691-700. doi: 10.1016/j.conbuildmat.2016.09.087